Structural Engineering and Mechanics, *Vol. 63, No. 1 (2017) 11-21*
DOI: https://doi.org/10.12989/sem.2017.63.1.011

Novel techniques for improving the interpolation functions of Euler-Bernoulli beam

Alireza A. Chekab[*1] and Ahmad A. Sani[2a]

[1]*Civil Engineering Department, Mashhad Branch, Islamic Azad University, Iran*
[2]*Civil Engineering Department, Ferdowsi University of Mashhad, Iran*

(Received May 16, 2016, Revised June 7, 2017, Accepted June 9, 2017)

Abstract. In this paper, the efficiency and the accuracy of classical (CE) and high order (HE) beam element are improved by introducing two novel techniques. The first proposed element (FPE) provides an alternative for (HE) by taking the mode shapes of the clamped-clamped (C-C) beam into account. The second proposed element (SPE) which could be utilized instead of (CE) and (HE) considers not only the mode shapes of the (C-C) beam but also some virtual nodes. It is numerically proven that the eigenvalue problem and the frequency response function for Euler-Bernoulli beam are obtained more accurate and efficient in contrast to the traditional ones.

Keywords: improved beam element; Clamped-Clamped beam mode shapes; virtual nodes; frequency response function

1. Introduction

Finite element method is one of the most powerful numerical approaches for obtaining approximate solution of boundary and initial value problems characterized by partial differential equations. Alongside this method, other robust numerical approaches such as differential quadrature, meshless, discrete singular convolution and so forth are widely used in various researches (Wang and Yuan 2017, Akgöz and Civalek 2015, Akgöz and Civalek 2014, Civalek *et al*. 2010, Civalek 2004, Liu and Wu 2001). From an engineering standpoint, finite element method is indispensably utilized for solving different problems such as stress analysis, heat transfer, fluid flow, and so on (Rao 2011, Reddy 2006, Cook *et al*. 1989, Hughes 1987). Although the finite element method is utilized in analyzing wide range of problems, this method is still being enhanced by increasing the accuracy and efficiency (Carrera *et al*. 2015, Li *et al*. 2015, Kim 2014, Dukić *et al*. 2014, Kazakov 2012). The accurate finite element analysis relies heavily on employing appropriate interpolation functions which represent the behavior of the solution within an element. In fact, interpolation functions of various orders and dimensions enable finite element approach to solve distinct types of problems with varying degrees of accuracy (Rao 2011). Subsequently, variety of researchers have been interested in this subject and proposed the new interpolation functions for solving different problems (Bishop 2014, Inaudi 2013). Milsted and Hutchinson (1974) presented the finite element solution to the membrane eigenvalue problem. They used polynomials plus trigonometric functions for constructing the interpolation functions. Trigonometric terms are utilized for additional degree of freedom to both boundary and interior nodes of the element. Augarde (1998) described the generation of Hermitian interpolation functions from Lagrangian interpolation polynomials and implemented many-noded straight beam elements within a finite element analysis code. Moreover, Hashemi and Richard (1999) presented a dynamic finite element formulation to calculate the natural frequencies and mode shapes of Euler-Bernoulli rotating beam by using the frequency dependent trigonometric interpolation functions. The interpolation functions of rotating beam finite element are developed by Gunda and Ganguli (2008) with satisfying the governing static homogenous differential equation of Euler-Bernoulli rotating beam. In this case, they are the functions of element length, rotational speed, element location across the beam, element mass and stiffness and length of the beam.

Since the free and forced vibrations of generally restrained beam (GRB) are considered in this study as numerical results, it is vital to pay attention to this subject in the literature. It should be pointed out that the vibration of beam with generally restrained supports is extensively investigated by researchers. For instance, Macbai and Genin (1973) presented the effects of elastic support on the natural frequencies of a built-in beam. Furthermore, the upper and lower bounds for the dynamic support stiffness are investigated. Grefi and Mittendorf (1976) introduced a method based on the discrete technique of component mode analysis for vibration analysis of a wide range of beams, plate and shell problems, including the effects of variable geometry and material properties. Besides, the problem of free vibration of Timoshenko beams with the elastically supported ends is solved by using a finite element model (Abbas 1984). Rao and Mirza (1989) derived the exact

*Corresponding author
E-mail: alireza.alipour.chekab@gmail.com
[a]Assistant Professor
E-mail: aftabi.ahmad@gmail.com

ISSN: 1225-4568 (Print), 1598-6217 (Online)

eigen-frequency equations for a wide range of restraint parameters of generally restrained Bernoulli-Euler beam. In addition, the applicability of the Fourier series to the dynamic analysis of beams having arbitrary boundary conditions investigated by Wang and Lin (1996). The numerical results for free vibration and dynamic response based on the Fourier series are compared with the results of conventional modal analysis. Kim and Kim (2001) derived the eigen-frequency equations of Euler-Bernoulli beams with general restraints in matrix form by using the Fourier series. This form could solve both the beam problems with generally restrained boundary conditions and the classical boundary conditions when appropriate restraint constants are assigned. On the basis of Green's function, Abu-Hilal (2003) presented the method for determining the dynamic response of damped Euler-Bernoulli beams.

In this paper, the usual procedures in finding the interpolation functions of the classical beam element (i.e., a two-node Hermite cubic element with two degrees of freedom per node, transverse displacement and rotation), is firstly expressed. In this method, the accuracy of beam element is increased by adding extra nodes or degrees of freedom. However, finding the interpolation functions would lead to cumbersome process due to need to symbolic inversing of a large parametric matrix which is denoted by [G]. The dimensions of this square matrix are equal to the number of degrees of freedom, including the values of polynomial, trigonometric or the other base functions or their derivatives in each node. To improve this process, two innovative approaches which are more efficient and straightforward in contrast to the conventional ones for constructing the interpolation functions are depicted. To show the accuracy and efficiency of two proposed methods, both free and forced vibration analysis of the generally restrained beam (GRB) are investigated. For this aim, the eigenvalue problem is solved for the various introduced beam elements and compared with exact ones. Furthermore, the dimensionless frequency parameter is obtained and classified into eight cases for different values of known spring constants. Afterwards, the exact frequency response function (FRF) under the vertical base excitation is presented for some verification purposes. It will be concluded that both proposed elements are more accurate and efficient in contrast to the traditional ones.

2. Classical Element (CE)

The beam element of length with two degrees of freedom per node is shown in Fig. 1. In what follows, the standard procedure for finding the interpolation functions is reviewed briefly. For this purpose, four arbitrary functions, which are often selected from polynomial functions, are chosen. The beam deflection function is approximated as a linear combination of four known functions with four unknown constants

$$U(x)=\begin{bmatrix} f_1(x) & f_2(x) & f_3(x) & f_4(x)\end{bmatrix}\begin{Bmatrix}\alpha_1\\ \alpha_2\\ \alpha_3\\ \alpha_4\end{Bmatrix} \tag{1}$$

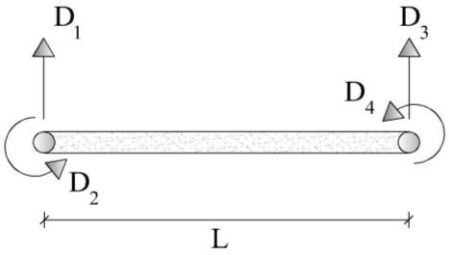

Fig. 1 Beam element with four degrees of freedom

which $U(x)$ is the deflection function of beam, $f_1(x)$ through $f_4(x)$ are four arbitrary base functions, α_1, α_2, α_3 and α_4 are four unknown constants. Eq. (1) can be rewritten as

$$U(x)=\left[f(x)\right]\{\alpha\} \tag{2}$$

which [$f(x)$] is the row matrix and usually defined as

$$\left[f(x)\right]=\begin{bmatrix}1 & x & x^2 & x^3\end{bmatrix} \tag{3}$$

also, $\{\alpha\}$ is the vector includes α_1 through α_4. Notice that the element under study has four degrees of freedom. As a result, by finding only four interpolation functions, $U(x)$ can be expressed as follows

$$U(x)=N_1(x)D_1+N_2(x)D_2+N_3(x)D_3+N_4(x)D_4 \tag{4}$$

or

$$U(x)=\left[N(x)\right]\{D\} \tag{5}$$

Where $N_i(i=1,4)$ are the interpolation functions and $D_j(j=1,4)$ are the degrees of freedom that could be defined as below

$$\begin{aligned} D_1&=U(0)=\left[f(0)\right]\{\alpha\}\\ D_2&=U'(0)=\left[f'(0)\right]\{\alpha\}\\ D_3&=U(L)=\left[f(L)\right]\{\alpha\}\\ D_4&=U'(L)=\left[f'(L)\right]\{\alpha\}\end{aligned} \tag{6}$$

Eq. (6) could be rewritten in matrix form by using Eq. (1)

$$\begin{Bmatrix}D_1\\ D_2\\ D_3\\ D_4\end{Bmatrix}=\begin{bmatrix} f_1(0) & f_2(0) & f_3(0) & f_4(0)\\ f_1'(0) & f_2'(0) & f_3'(0) & f_4'(0)\\ f_1(L) & f_2(L) & f_3(L) & f_4(L)\\ f_1'(L) & f_2'(L) & f_3'(L) & f_4'(L)\end{bmatrix}\begin{Bmatrix}\alpha_1\\ \alpha_2\\ \alpha_3\\ \alpha_4\end{Bmatrix} \tag{7}$$

Consequently

$$\{D\}=\left[G\right]\{\alpha\} \tag{8}$$

where [G] is coefficient matrix

$$\left[G\right]=\begin{bmatrix}1 & 0 & 0 & 0\\ 0 & 1 & 0 & 0\\ 1 & L & L^2 & L^3\\ 0 & 1 & 2L & 3L^2\end{bmatrix} \tag{9}$$

Subsequently

$$\{\alpha\} = [G]^{-1}\{D\} \tag{10}$$

substituting Eq. (10) into Eq. (2) gives

$$U(x) = [f(x)]\,[G]^{-1}\{D\} \tag{11}$$

comparing Eq. (11) with Eq. (5) yields

$$[N(x)] = [f(x)]\,[G]^{-1} \tag{12}$$

The complicated and time-consuming step in process of finding the interpolation functions is devoted to find the inverse of the coefficient matrix [*G*]. In addition, the inversion process should be generally carried out in parametric form, and coefficient matrices with large dimensions provide some limitations for parametric calculations. Considering additional nodes, the size of [*G*] will be increased, as a result of which the inverse of this matrix is obtained strenuously. The stiffness and mass matrices of individual element is defined based on the interpolation functions as follows (Reddy 2006)

$$\begin{aligned} K_{ij} &= \int_0^L N_i''(x)\,EI(x)\,N_j''(x)\,dx \\ M_{ij} &= \int_0^L N_i(x)\,\rho A(x)\,N_j(x)\,dx \end{aligned} \tag{13}$$

EI, ρ, *A* in this relation represent the flexural rigidity, mass density and the cross-sectional area of the beam. In the next step, the accuracy of beam element is increased by adding inner equidistant nodes with 2 degree of freedom at each node.

3. High order beam element (HE)

One of the usual approaches for increasing the accuracy of beam element is adding inner equidistant nodes with 2 degree of freedom at each node. Herein, a four-node element with eight bending degrees of freedom and a total length of *L* is shown in Fig. 2. In this case, complete polynomial of order seven is chosen due to the fact that the four additional degrees of freedom are considered. Hence

$$[f(x)] = \begin{bmatrix} 1 & x & x^2 & x^3 & x^4 & x^5 & x^6 & x^7 \end{bmatrix} \tag{14}$$

Herein, [*G*] would be a 8×8 matrix which is defined as follows

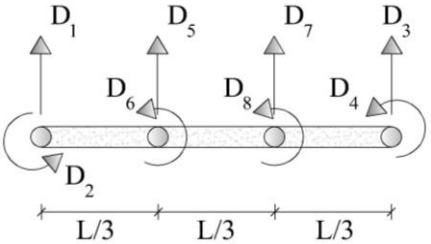

Fig. 2 Beam element with eight degrees of freedom

$$[G] = \left[\begin{array}{cccc:cccc} 1 & 0 & 0 & 0 & 0 & 0 & 0 & 0 \\ 0 & 1 & 0 & 0 & 0 & 0 & 0 & 0 \\ 1 & L & L^2 & L^3 & L^4 & L^5 & L^6 & L^7 \\ 0 & 1 & 2L & 3L^2 & 4L^3 & 5L^4 & 6L^5 & 7L^6 \\ \hdashline 1 & \frac{L}{3} & \left(\frac{L}{3}\right)^2 & \left(\frac{L}{3}\right)^3 & \left(\frac{L}{3}\right)^4 & \left(\frac{L}{3}\right)^5 & \left(\frac{L}{3}\right)^6 & \left(\frac{L}{3}\right)^7 \\ 0 & 1 & 2\left(\frac{L}{3}\right) & 3\left(\frac{L}{3}\right)^2 & 4\left(\frac{L}{3}\right)^3 & 5\left(\frac{L}{3}\right)^4 & 6\left(\frac{L}{3}\right)^5 & 7\left(\frac{L}{3}\right)^6 \\ 1 & \left(\frac{2L}{3}\right) & \left(\frac{2L}{3}\right)^2 & \left(\frac{2L}{3}\right)^3 & \left(\frac{2L}{3}\right)^4 & \left(\frac{2L}{3}\right)^5 & \left(\frac{2L}{3}\right)^6 & \left(\frac{2L}{3}\right)^7 \\ 0 & 1 & 2\left(\frac{2L}{3}\right) & 3\left(\frac{2L}{3}\right)^2 & 4\left(\frac{2L}{3}\right)^3 & 5\left(\frac{2L}{3}\right)^4 & 6\left(\frac{2L}{3}\right)^5 & 7\left(\frac{2L}{3}\right)^6 \end{array}\right] \tag{15}$$

The above matrix consists of four blocks, and each block is comprised of a 4×4 matrix. As it is shown in Eq. (9), the first block of this matrix is exactly similar to the [*G*] which is obtained for classical beam element when four degrees of freedom are considered. According to Eq. (12), for obtaining the interpolation functions of eight degrees of freedom element, the inverse of matrix (15) must be attained through cumbersome symbolic computations. Obviously, this procedure becomes complicated when the degrees of freedom are increased. If the added functions, which are pertinent to the additional degrees of freedom, D_5 through D_8, are taken into consideration in such a way that the upper right matrix block becomes completely zero, the inverse of 8×8 matrix would be reduced to inverse of two 4×4 matrices. In fact, if the interior nodes are still located at $x=L/3$ and $x=2L/3$ as shown in Fig. 2, and the terms of the additional base functions are chosen different from x^4 through x^8, the inverse of [*G*] would be obtained conveniently. Recall that, the inverse of partitioned matrix

$$[A] = \left[\begin{array}{c:c} B & 0 \\ \hdashline C & D \end{array}\right] \tag{16}$$

is attained straightforwardly as below (Anton and Rorres 2005)

$$[A]^{-1} = \left[\begin{array}{c:c} B^{-1} & 0 \\ \hdashline -DCB^{-1} & D^{-1} \end{array}\right] \tag{17}$$

It can be seen that for inversing the main matrix [*A*] it is just necessary to find out the inverse of two sub-matrices [*B*] and [*D*]. In contrast to the inverse of 8×8 matrix, the inverse of two 4×4 matrices is carried out more convenient. According to Eq. (17), first proposed element is introduced in the next section.

4. First Proposed Element (FPE)

As mentioned before, the upper right matrix block [*G*] becomes zero if the additional base functions correspond to the added degrees of freedom are appropriately selected. This block consists of the values of added functions and their first derivatives at the ends of the beam. Instead of considering x^4, x^5, x^6 and x^7, $g_1(x)$ through $g_4(x)$ are selected. Consequently, [*f*(*x*)] for the element with eight degrees of freedom is defined as follows

$$[f(x)] = \left[\begin{array}{cccc:cccc} 1 & x & x^2 & x^3 & g_1(x) & g_2(x) & g_3(x) & g_4(x) \end{array}\right] \tag{18}$$

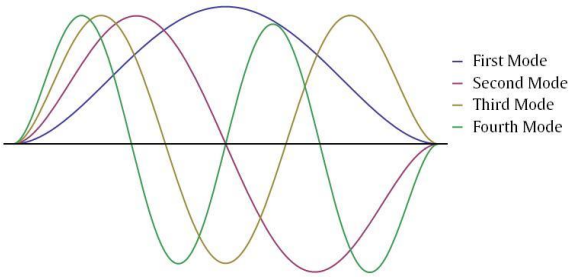

Fig. 3 Four mode shapes of clamped-clamped (C-C) beam

the upper right matrix block which must be set to zero is

$$\begin{bmatrix} g_1(0) & g_2(0) & g_3(0) & g_4(0) \\ g_1'(0) & g_2'(0) & g_3'(0) & g_4'(0) \\ g_1(L) & g_2(L) & g_3(L) & g_4(L) \\ g_1'(L) & g_2'(L) & g_3'(L) & g_4'(L) \end{bmatrix} = \left[0\right]_{4\times 4} \quad (19)$$

Generally, various functions could be found in such a way that the values of $g_i(x)$ and their first derivatives at x=0 and x=L become zero. It is valuable if a set of functions with a remarkable physical interpretation are found. One of the most important functions which have these characteristics, are the mode shapes of the clamped-clamped (C-C) beam.

Each arbitrary deflection function of the beams could be expanded by the set of linear independent functions called orthogonal eigenfunctions. One of the most well-known eigenfunctions of the structures is the dynamic mode shapes. For instance, in this case, it seems sufficient to consider only the first four mode shapes from the set of infinite mode shapes of the clamped-clamped (C-C) beam. The first four mode shapes of clamped-clamped (C-C) beam are plotted in Fig. 3.

Considering $g_1(x)$ through $g_4(x)$ as four mode shapes of the C-C beam (but not definitely the first ones), the upper right matrix block of [G] which is shown in Eq. (19), would be become zero. For obtaining the mode shapes of the clamped-clamped (C-C) beam, the free vibration equation must be solved analytically as follows

$$\frac{d^4U}{dx^4} - \lambda^4 U = 0 \quad (20)$$

in which $\lambda^4 = \frac{\omega^2 \rho A}{EI}$, and λL is defined as the dimensionless frequency parameter of the beam. Solving Eq. (19) yields

$$U(x) = A\,Sin\,\lambda x + B\,Cos\,\lambda x + C\,Sinh\,\lambda x + D\,Cosh\,\lambda x \quad (21)$$

where, A, B, C and D are four unknown constants. Imposing the boundary conditions at x=0, i.e., $U(0) = U'(0) = 0$, leads to

$$\begin{cases} D = -B \\ C = -A \end{cases} \quad (22)$$

therefore, $U(x)$ is rewritten as below

$$U(x) = A\left(Sin\,\lambda x - Sinh\,\lambda x\right) + B\left(Cos\,\lambda x - Cosh\,\lambda x\right) \quad (23)$$

Applying the boundary conditions at x=L, i.e., $U(L) = U'(L) = 0$, yields

$$\begin{bmatrix} Sin\,\lambda L - Sinh\,\lambda L & Cos\,\lambda L - Cosh\,\lambda L \\ Cos\,\lambda L - Cosh\,\lambda L & -Sin\,\lambda L - Sinh\,\lambda L \end{bmatrix} \begin{Bmatrix} A \\ B \end{Bmatrix} = \begin{Bmatrix} 0 \\ 0 \end{Bmatrix} \quad (24)$$

In order to have a nontrivial solution, the determinant of the coefficient matrix is set equal to zero. This equation could be simplified as

$$Cos\,\lambda L = \frac{1}{Cosh\,\lambda L} \quad (25)$$

By solving Eq. (25), the first four dimensionless parameters λL would be obtained as follows

$$\lambda_1 = \frac{4.7300407448}{L},\ \lambda_2 = \frac{7.8532046240}{L},$$
$$\lambda_3 = \frac{10.9956078380}{L},\ \lambda_4 = \frac{14.1371654912}{L},\ldots \quad (26)$$

by identifying λL, the determinant of the coefficient matrix of Eq. (24) is equal to zero and the two equations become linearly dependent. In this case, A and B are dependent on each other. For instance, by assuming $B = \xi A$ the second equation could be written as follows

$$\left(Cos\,\lambda L - Cosh\,\lambda L\right)A - \left(Sin\,\lambda L - Sinh\,\lambda L\right)\xi A = 0, \quad (27)$$

subsequently

$$\xi = \frac{Cos\,\lambda L - Cosh\,\lambda L}{Sin\,\lambda L - Sinh\,\lambda L} \quad (28)$$

Now, $U(x)$ are the mode shapes of clamped-clamped (C-C) beam. Hence

$$U(x) = A\left[\left(Sin\,\lambda x - Sinh\,\lambda x\right) + \frac{Cos\,\lambda L - Cosh\,\lambda L}{Sin\,\lambda L - Sinh\,\lambda L}\left(Cos\,\lambda x - Cosh\,\lambda x\right)\right] \quad (29)$$

Notify that the attained functions are the mode shapes of the C-C beam if and only if the λ parameters are equal to the beam frequency parameters introduced in Eq. (26). Subsequently the four suggested functions $g_1(x)$ through $g_4(x)$ become

$$g_i(x) = \left[Sin\left(r_i\frac{x}{L}\right) - Sinh\left(r_i\frac{x}{L}\right)\right] + \left(\frac{Cos\,r_i - Cosh\,r_i}{Sin\,r_i - Sinh\,r_i}\right)\left[Cos\left(r_i\frac{x}{L}\right) - Cosh\left(r_i\frac{x}{L}\right)\right] \quad (30)$$

where $r_i = \lambda L$. Notice in particular that the values of $g_i(x)$ and their first derivatives at x=0 and x=L are equal to zero. Therefore, if the functions $g_1(x)$ through $g_4(x)$ are considered as the additional base functions in [$f(x)$], the upper right matrix block coefficient matrix becomes completely zero. As a result, the procedure of inversing [G] becomes perfectly simple and efficient. In fact, in the process of inversing the coefficient matrix, the upper right matrix block becomes zero

$$\left[G\right] = \left[\begin{array}{c|c} G_B & 0 \\ \hline G_C & G_I \end{array}\right] \quad (31)$$

utilizing Eq. (17) gives

$$\left[G\right]^{-1}=\left[\begin{array}{c|c} G_B^{-1} & 0 \\ \hline -G_I^{-1}G_C\,G_B^{-1} & G_I^{-1} \end{array}\right] \tag{32}$$

where $[G_B]$ is the 4×4 matrix which is germane to the standard polynomials, $[G_I]$ is the 4×4 matrix which is consist of $g_1(x)$ through $g_4(x)$, and $[G_c]$ is mixed of two sub-matrices. Recall that, $[N(x)]$ are obtained through Eq. (12). The ith additional interpolation function (i=5,…,8) could be found by multiplying the new $[f(x)]$ by the column of $[G]^{-1}$ from Eq. (31)

$$N_i(x)=\left[\begin{array}{cccc|cccc} 1 & x & x^2 & x^3 & g_1(x) & g_2(x) & g_3(x) & g_4(x) \end{array}\right]\left\{\begin{array}{c} 0 \\ 0 \\ 0 \\ 0 \\ G_I^{-1}(5,i) \\ G_I^{-1}(6,i) \\ G_I^{-1}(7,i) \\ G_I^{-1}(8,i) \end{array}\right\} \tag{33}$$

Eq. (33) clearly shows that the upper right matrix block is equal to zero, and the additional interpolation functions are only depended on the new base functions $g_i(x)$. Interestingly, the mode shapes of the simple structures are orthogonal. In this case, two different mode shapes of the beam with the length of L are orthogonal in the interval $0\le x\le L$

$$\int_0^L g_i(x)\,g_j(x)\,dx=0 \qquad i\neq j \tag{34}$$

In this stage, it is noteworthy to find out where this property could be helpful. The mass matrix $[M^e]$ of the element could be expressed as

$$\left[M^e\right]=\rho A\left[G\right]^{-T}\int_0^L\left[f(x)\right]^T\left[f(x)\right]dx\,\left[G\right]^{-1} \tag{35}$$

the superscript T over $[f(x)]$ indicates matrix transpose. Eq. (35) is rewritten as follows

$$\left[M^e\right]=\rho A\left[G\right]^{-T}\left[m\right]\left[G\right]^{-1} \tag{36}$$

Note that the general component of the mass matrix which is related to the additional degrees of freedom could be stated as

$$m_{ij}=\int_0^L f_i(x)f_j(x)\,dx=\int_0^L g_{i-4}(x)\,g_{j-4}(x)\,dx=\int_0^L g_k(x)\,g_n(x)\,dx \tag{37}$$

where $i,j=5$ to 8, $k=i-4$ and $n=j-4$. If $k\neq n$ Eq. (37) becomes to zero, and as a result of which, the 4×4 lower right block of mass matrix which is related to the four additional degrees of freedom becomes diagonal. Herein, the stiffness matrix could be rewritten by utilizing Eqs. (12) and (13) as

$$\left[K^e\right]=EI\left[G\right]^{-T}\left(\int_0^L\left[f''(x)\right]^T\left[f''(x)\right]dx\right)\left[G\right]^{-1} \tag{38}$$

the superscript T over $\left[f''(x)\right]$ indicates matrix transpose. Simplifying Eq. (38) yields

$$\left[K^e\right]=EI\left[G\right]^{-T}\left[k\right]\left[G\right]^{-1} \tag{39}$$

The new defined 8×8 matrix $[k]$ is the integration of the transpose of the second derivative row matrix $[f(x)]$ which is multiplied by itself. The second derivative of $[f(x)]$ is stated as follows

$$\left[f(x)''\right]=\left[\begin{array}{cccc|cccc} 0 & 0 & 2 & 6x & g_1''(x) & g_2''(x) & g_3''(x) & g_4''(x) \end{array}\right] \tag{40}$$

Notice that, if the beam is modeled by employing only one element, the eigenvalue problem would be stated as below

$$\left[K^e\right]\{X\}=\omega^2\left[M^e\right]\{X\} \tag{41}$$

where $\{X\}$ represented the eigenvector and ω is the circular frequency. Substituting Eqs. (36) and (39) into (41), gives

$$EI\left[G\right]^{-T}\left[k\right]\left[G\right]^{-1}\{X\}=\rho A\,\omega^2\left[G\right]^{-T}\left[m\right]\left[G\right]^{-1}\{X\} \tag{42}$$

Eq. (42) could be rewritten as below

$$\left[G\right]^{-T}\left(EI\left[k\right]-\omega^2\rho A\left[m\right]\right)\left[G\right]^{-1}\{X\}=\{0\} \tag{43}$$

by defining

$$\left[G\right]^{-1}\{X\}=\{Y\} \tag{44}$$

the new eigenvalue problem in terms of $[k]$ and $[m]$ matrices can be stated as follows

$$\left[G\right]^{-T}\left(EI\left[k\right]-\omega^2\rho A\left[m\right]\right)\{Y\}=\{0\} \tag{45}$$

where $\{Y\}$ is the new eigenvector. In order to find the nontrivial solution, the determinant of the coefficient matrix is set equal to zero. Therefore, the natural frequencies are obtained by solving the following equation

$$Det\left|\left[k\right]-\frac{\omega^2\rho A}{EI}\left[m\right]\right|=0 \tag{46}$$

substituting $\lambda^4=\omega^2\rho A/EI$ into Eq. (46) gives

$$Det\left|\left[k\right]-\lambda^4\left[m\right]\right|=0 \tag{47}$$

4. Second Proposed Element (SPE)

In this section, the second proposed element for improving the classical beam element (CE) and enhancing high order element (HE) is presented. Furthermore, it is explained how this novel technique is efficient in contrast to the previous ones. In this approach, the interpolation functions of the traditional beam element are enhanced by employing m mode shapes of the C-C beam. The fundamental concept of this technique could be clarified as follows

$$U(x)=\alpha_1+\alpha_2 x+\alpha_3 x^2+\alpha_4 x^3+\sum_{j=1}^{m}\alpha_{j+4}\,g_j(x) \qquad (48)$$

it can be seen that the first four terms of Eq. (48) are the approximating functions which are utilized in classical element (CE). The main four degrees of freedom of the beam element can be expressed as follows

$$\begin{aligned}
D_1 &= U(0)=\alpha_1 &&+\sum_{j=1}^{m}\alpha_{j+4}\,g_j(0)\\
D_2 &= U'(0)=\alpha_2 &&+\sum_{j=1}^{m}\alpha_{j+4}\,g_j'(0)\\
D_3 &= U(L)=\alpha_1+\alpha_2 L+\alpha_3 L^2+\alpha_4 L^3+ &&\sum_{j=1}^{m}\alpha_{j+4}\,g_j(L)\\
D_4 &= U'(L)=\alpha_2+2\alpha_3 L+3\alpha_4 L^2+ &&\sum_{j=1}^{m}\alpha_{j+4}\,g_j'(L)
\end{aligned} \qquad (49)$$

Recall that, the terms which are situated in sigma are equal to zero while the boundary conditions of clamped-clamped (C-C) beam are imposed on $g_j(x)$. Consequently, up to this stage

$$\begin{Bmatrix} D_1\\ D_2\\ D_3\\ D_4 \end{Bmatrix}=\left[G_B\right]\begin{Bmatrix} \alpha_1\\ \alpha_2\\ \alpha_3\\ \alpha_4 \end{Bmatrix} \qquad (50)$$

The m virtual degrees of freedoms are defined as

$$D_5=\alpha_5;\ D_6=\alpha_6;\cdots;\ D_m=\alpha_m, \qquad (51)$$

or

$$\begin{Bmatrix} D_5\\ D_6\\ \cdot\\ \cdot\\ \cdot\\ D_m \end{Bmatrix}=\left[I\right]\begin{Bmatrix} \alpha_5\\ \alpha_6\\ \cdot\\ \cdot\\ \cdot\\ \alpha_m \end{Bmatrix} \qquad (52)$$

where [I] is an identity matrix which is consist of (m-4) rows and columns. Interestingly, it is unrecognizable what D_5 through D_m are, and where their locations are. Based on the expressions given for m virtual degrees of freedom, the coefficient matrix which is pertinent to the new beam element could be expressed as follows

$$\left[G\right]=\left[\begin{array}{c|c} G_B & 0\\ \hline 0 & I \end{array}\right] \qquad (53)$$

inversing the above matrix yields

$$\left[G\right]^{-1}=\left[\begin{array}{c|c} G_B^{-1} & 0\\ \hline 0 & I \end{array}\right] \qquad (54)$$

In this case, the above partitioned matrix is consisting of two sub-matrices with zero values. As mentioned before, finding the inverse of the coefficient matrix is a time-consuming and cumbersome step. Due to the simple nature of Eq. (53) the inverse of this matrix is readily attained by reducing the computational efforts. Therefore, the first four interpolation functions are strikingly similar to N_1 to N_4 for the classical element. It must be emphasized that the (m-4) new functions are definitely the mode shapes of clamped-clamped beam.

5. Numerical results

This section deals with the computational performance of discussed elements, and their applications for the free and forced vibration of generally restrained Euler-Bernoulli beam. The finite element results will be compared with analytical solutions. For this purpose, first, the eigenvalue problem is solved for the presented beam elements and compared with exact eigenvalues. Afterwards, the exact frequency response function (FRF) of generally restrained beam (GRB) is obtained in frequency domain. Afterwards, the frequency response functions for both exact and finite element solutions are plotted. Comparisons are made through the convergence of elements to exact natural frequencies for each mode. In addition, the frequency response functions are attained for different values of non-dimensional frequency parameter. Consequently, the capability and robustness of two proposed elements will be examined.

5.1 Free vibration

A straight uniform Euler-Bernoulli beam of length L, partially restrained against translation and rotation at its ends is shown in Fig. 4. The translational restraint is characterized by $K_1=\alpha EI/L^3$ at one end and $K_3=\gamma EI/L^3$ at the other end, and the rotational restraint $K_2=\beta EI/L$ and $K_4=\delta EI/L$. Moreover, α, β, γ and δ are the arbitrary known dimensionless stiffness constants.

Solving eigenvalue problem for different elements would lead to the values of the non-dimensional frequency parameter (λL). In the following problems, for the SPE element, the number of virtual degrees of freedom (m) equal four. Considering only one element, the results for the first four modes for different values of α, β, γ and δ are classified into 8 cases. Although a wide range of numerical results have been generated, due to space limitations, only a few cases are presented in this paper. Tables 1-8 include the

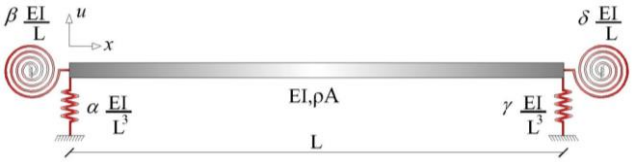

Fig. 4 Geometry of generally restrained Bernoulli-Euler beam

Table 1 Case 1: Values of the dimensionless frequency parameter (λL) for α, γ=0.1 and β, δ=0.1

	Various Methods				
Mode	Exact	CE	HE	FPE	SPE
1	0.6684728889	0.668519285	0.6684728889	0.6684729132	0.6684729132
2	1.3092120493	1.309327213	1.309212046	1.3092127235	1.3092127236
3	4.7715490482	5.245344392	4.771574272	4.7725636693	4.7725636692
4	7.8787172144	9.630819671	7.879745955	7.8824131545	7.8824131545

Table 2 Case 2: Values of the dimensionless frequency parameter (λL) for α, γ=0.1 and β, δ=100

	Various Methods				
Mode	Exact	CE	HE	FPE	SPE
1	0.6686893152	0.6687357521	0.6686893148	0.6686893395	0.6686893395
2	3.1142982891	3.12507341	3.1142982901	3.114340473	3.1143404739
3	6.2232960253	13.84294919	6.2242032152	6.226801935	6.2268019353
4	9.3357758982	21.46549391	9.3455676753	9.346414593	9.3464145938

Table 3 Case 5: Values of the dimensionless frequency parameter (λL) for α, γ=1 and β, δ=0.1

	Various Methods				
Mode	Exact	CE	HE	FPE	SPE
1	1.184478676	1.185296618	1.184478676	1.184479091	1.184479091
2	1.696265304	1.696687067	1.696265304	1.696267766	1.696267766
3	4.787948788	5.260910369	4.787974789	4.788989954	4.788989954
4	7.882388043	9.634358521	7.883421437	7.886106589	7.886106589

Table 4 Case 4: Values of the dimensionless frequency parameter (λL) for α, γ=1 and β, δ=100

	Various Methods				
Mode	Exact	CE	HE	FPE	SPE
1	1.188300928	1.189126169	1.188300927	1.188301357	1.188301357
2	3.144179614	3.155490843	3.144179615	3.144223816	3.144223816
3	6.227220149	13.84379736	6.228131708	6.230744436	6.230744436
4	9.336969875	21.46585364	9.346772319	9.347624315	9.347624315

Table 5 Case 5: Values of the dimensionless frequency parameter (λL) for α, γ=10 and β, δ=0.1

	Various Methods				
Mode	Exact	CE	HE	FPE	SPE
1	2.035385162	2.048648027	2.035385162	2.035390261	2.035390261
2	2.788458341	2.793675281	2.788458342	2.788487102	2.788487102
3	4.947253452	5.412782769	4.947288236	4.948569641	4.948569641
4	7.919256312	9.669771484	7.920337348	7.923204915	7.923204915

values of natural frequencies for each mode based on the exact and finite element solutions in terms of the stiffness dimensionless parameters α, β, γ and δ. Note that the exact solutions are coincided with those which are obtained for different cases in Rao and Mirza (1989) research.

Table 6 Case 6: Values of the dimensionless frequency parameter (λL) for α, γ=10 and β, δ=100

	Various Methods				
Mode	Exact	CE	HE	FPE	SPE
1	2.098729773	2.113304417	2.098729774	2.098736776	2.098736776
2	3.403000098	3.419935492	3.403000106	3.403064984	3.403064984
3	6.266456738	13.85227505	6.267412867	6.270166423	6.270166423
4	9.348933151	21.46945064	9.358842872	9.359745596	9.359745596

Table 7 Case 7: Values of the dimensionless frequency parameter (λL) for α, γ=100 and β, δ=0.1

	Various Methods				
Mode	Exact	CE	HE	FPE	SPE
1	2.896361262	2.996510813	2.896361329	2.896370644	2.896370644
2	4.663805665	4.751257368	4.663806197	4.664087977	4.664087977
3	6.086465167	6.580700096	6.086728201	6.090825292	6.090825292
4	8.294713915	10.02351552	8.296390726	8.301280535	8.301280535

Table 8 Case 8: Values of the dimensionless frequency parameter (λL) for α, γ=100 and β, δ=100

	Various Methods				
Mode	Exact	CE	HE	FPE	SPE
1	3.497751893	3.735294995	3.497752558	3.497805126	3.497805126
2	4.664729852	4.753443275	4.664730387	4.665008471	4.665008471
3	6.648886375	13.93664575	6.650379057	6.654544459	6.654544459
4	9.470610645	21.50539104	9.481654171	9.483056659	9.483056659

The dimensionless natural frequencies which are presented in Tables 1-8 show that the results of HE element and two proposed elements are estimate the exact solution desirably, although the former gives better estimation in almost all tables in contrast to the proposed elements when considering only one element. However, it is important to notice that these elements estimate exact solution with diminishing the time-consuming steps of computation as mentioned before, in contrast to the former. In Case 1-2 the coefficient of translational spring are constant and equal to 0.1; moreover, the values of rotational stiffness are slightly increased. Similarly, in Cases 3-4, Cases 5-6 and Cases 7-8 the coefficient of translational spring values are constant and equal to 1, 10,100, respectively and the rotational stiffness are varied gradually. Although the translational and rotational stiffness increase the dimensionless frequency parameter λL, this influence is relatively greater for translational springs.

In Case 7, the stiffness of rotational springs are negligible, as a result of which this beam is similar to the simple-simple (S-S) beam. However, the corresponding values of λL are relatively smaller than (S-S) beam. In order to show the sensitivity analysis much better, Case 8 is selected. Although the stiffness of springs in Table 8 can be assumed as a model of clamped-clamped (C-C) beam, the

Table 9 Normalized eigen-values for the first mode of different elements

Number of Elements	CE	HE	FPE	SPE
1	1.006516145	1	1.000002505	1.000002505
2	1.000377701	1	1.000000187	1.000000187
3	1.000074002	1	1.000000038	1.000000038
4	1.000074002	1	1.000000038	1.000000038
5	1.000023353	1	1.000000012	1.000000012
6	1.000004605	1	1.000000002	1.000000002
7	1.000002485	1	1.000000001	1.000000001
8	1.000001456	1	1	1
9	1.000000909	1	1	1
10	1.000000596	1	1	1
⋮	⋮	⋮	⋮	⋮
20	1.000000037	Solution Diverge	1	1

Table 10 Normalized eigen-values for the fourth mode of different elements

Number of Elements	CE	HE	FPE	SPE
1	1.221045399	1.000136507	1.000498608	1.000498608
2	1.066450581	1.000000615	1.000035283	1.000035283
3	1.002499954	1.000000001	1.000007659	1.000007659
4	1.003213721	1	1.000002192	1.000002192
5	1.003213721	1	1.000002191	1.000002191
6	1.000875201	1	1.000000482	1.000000482
7	1.000498204	1	1.000000269	1.000000269
8	1.000301771	1	1.000000162	1.000000162
9	1.000192544	1	1.000000102	1.000000102
10	1.000128273	1	1.000000068	1.000000068
⋮	⋮	⋮	⋮	⋮
20	1.000008406	Solution Diverge	1	1

values of λL for the clamped-clamped beam (C-C) as shown in Eq. (26) are greater than Case 8. Besides, by considering Case 5 and dividing the beam into 20 elements the dimensionless frequency parameter λL is computed for various numbers of elements and compared with the exact solutions. The results are normalized with respect to the exact values and classified into two tables for first and four modes.

Convergence curves for Tables 9-10 are plotted in Figs. 5-6 as a function of the number of elements. In these figures, the values of classical element (CE) are approximately estimating the exact solutions. Increasing the number of the elements, the high order element (HE) rapidly converges to the exact values in contrast to the classical element (CE). It could be observed in Figs. 5-6, the trend of high order element is altered when the number of the elements are increased, reaching between 15 and 16. This means that, the values of dimensionless frequency

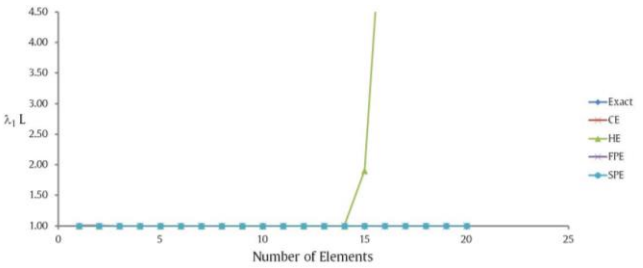

Fig. 5 **C**onvergence curves for the first mode

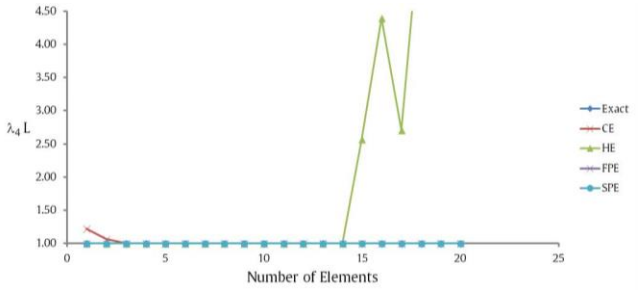

Fig. 6 Convergence curves for fourth mode

parameter instead of plummeting are increasing due to numerical errors. Therefore, it seems that the high order element (HE) beam elements with the small length are unstable for employing in the Euler-Bernoulli eigenvalue problem. As a result, instead of using high order element (HE), the first proposed element (FPE) could be utilized. Besides, it could be observed in Tables 9-10 when the beam element is divided to 8 elements, the (FPE) strongly converges to exact values. As mentioned before, (SPE) can be employed instead of (CE) since the exact solutions are estimated accurately by (SPE) due to virtual nodes which are used in this element. Furthermore, as it is shown in Figs. 5-6, (SPE) is also able to be employed instead of the high order element (HE), since the former could estimate the exact solutions more accurate in contrast to the latter with reducing more additional calculation and provides higher computational efficiency.

5.2 Forced vibration

In this stage, the exact frequency response function of generally restrained Euler-Bernoulli beam is obtained by solving the governing differential equation of the beam. The governing differential equation could be expressed in the time domain as follows

$$\frac{\partial^2}{\partial x^2}\left(EI\frac{\partial^2 u(x,t)}{\partial x^2}\right)+\rho A\frac{\partial^2 u_T(x,t)}{\partial t^2}=0 \tag{55}$$

In this relation, $u(x, t)$ is the transverse relative deflection of beam and $u_T(x, t)$ is the total deflection of the beam which is defined as follows

$$u_T(x,t)=u_g(x,t)+u(x,t) \tag{56}$$

where $u_g(x, t)$ is the displacement of ground. From a mathematical standpoint, Eq. (55) is a partial differential

equation (PDE) which can be transformed into frequency domain with the aid of integral transforms. For this aim, one of the most well-known of them, the Fourier transform, is utilized. The Fourier transform with respect to t can be defined as below

$$\mathbf{F}[f(x,t)]=\frac{1}{\sqrt{2\pi}}\int_{-\infty}^{+\infty} f(x,t)e^{-i\omega t}dt \tag{57}$$

where t and ω are time and frequency independent variables, respectively. Besides, **F** represents Fourier transform. Applying this transform into Eq. (55), yields

$$EI\mathbf{F}\left[\frac{\partial^4 u}{\partial x^4}\right]+\rho A\,\mathbf{F}\left[\frac{\partial^2}{\partial t^2}(u+u_g)\right]=0 \tag{58}$$

For harmonic ground excitation with the frequency ω, $\ddot{u}_g(x,t)=a_g(x,\omega)e^{i\omega t}$. By assuming $a_g(x,\omega)=1$, the Eq. (58) could be written as follows

$$EI\ \frac{d^4U(x,\omega)}{dx^4}-\rho A\,\omega^2 U(x,\omega)=-\rho A \tag{59}$$

Eq. (59) is the fourth order linear non-homogeneous ordinary differential equation (ODE). The complementary and the particular solutions of this equation are obtained as below

$$\begin{cases} U_c(x,\omega)=c_1 Sin\,\lambda x+c_2 Cos\,\lambda x+c_3 Sinh\,\lambda x+c_4 Cosh\,\lambda x \\ U_p(x,\omega)=\dfrac{1}{\omega^2} \end{cases} \tag{60}$$

therefore

$$U(x,\omega)=U_c(x,\omega)+U_p(x,\omega) \tag{61}$$

where $\lambda=(\omega^2\rho A/EI)^{1/4}$ is the eigen-frequency parameter of the beam. Imposing four boundary conditions, four constants c_1 through c_4 are obtained. The boundary conditions at x=0 are

$$\begin{cases} K_1U(0)+EIU'''(0)=0 \\ K_2U'(0)-EIU''(0)=0 \end{cases} \tag{62}$$

Boundary conditions at x=L gives

$$\begin{cases} K_3U(L)-EIU'''(L)=0 \\ K_4U'(L)+EIU''(L)=0 \end{cases} \tag{63}$$

in this relation K_1 through K_4 are the stiffness of springs which are defined as follows

$$K_1=\alpha\frac{EI}{L^3},K_2=\beta\frac{EI}{L},K_3=\gamma\frac{EI}{L^3},K_4=\delta\frac{EI}{L} \tag{64}$$

where α, β, γ and δ are the known dimensionless parameters. Imposing the boundary conditions (62) and (63) in Eq. (61) gives

$$\begin{bmatrix} -\mu^3 & \alpha & \mu^3 & \alpha \\ \beta & \mu & \beta & -\mu \\ \gamma Sin\,\mu+\mu^3 Cos\,\mu & \gamma Cos\,\mu-\mu^3 Sin\,\mu & \gamma Sinh\,\mu-\mu^3 Cosh\,\mu & \gamma Cosh\,\mu-\mu^3 Sinh\,\mu \\ \delta Cos\,\mu-\mu Sin\,\mu & -\delta Sin\,\mu-\mu Cos\,\mu & \delta Cosh\,\mu+\mu Sinh\,\mu & \delta Sinh\,\mu+\mu Cosh\,\mu \end{bmatrix}\begin{Bmatrix} c_1 \\ c_2 \\ c_3 \\ c_4 \end{Bmatrix}=\begin{Bmatrix} \alpha \\ 0 \\ \gamma \\ 0 \end{Bmatrix} \tag{65}$$

where μ=λL is another dimensionless coefficient. Solving the system of equations, Eq. (65), the unknown coefficients c_1 through c_4 are obtained. Afterwards, the frequency response functions (FRF) are plotted for various elements. In each case, the slope of the beam at x=0 is plotted against the dimensionless frequency parameter. The dimensionless frequency parameter is defined as ω/ω_1^s, where ω is the excitation frequency and ω_1^s represents the fundamental frequency of the beam for the symmetric modes. Results are obtained for different number of elements by employing (CE), (HE), (FPE) and (SPE) elements. Assuming α=10, β=0.1, γ=10, δ=0.1 and various number of elements (*NE*), different analyzes are done for the different values of ω/ω_1^s, as follows.

It can be seen from the Fig. 7, the high order element and both proposed elements are estimated the exact solutions more accurate in contrast to the classical element. Since the SPE is an alternative element for CE and HE, and the results are the same for HE and SPE, the accuracy of the SPE is shown in Fig. 8 in comparison to the CE element. It could be observed that the SPE element can estimate the exact solutions with only one element in contrast to CE which is able to estimate the exact results when the number of elements are increased, reaching eight elements. Although increasing the number of elements may reduce the

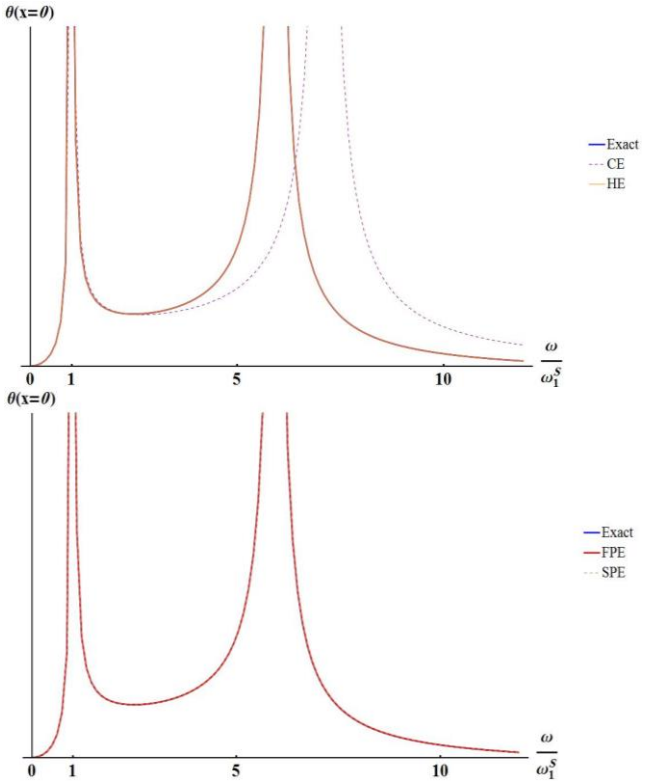

Fig. 7 FRFs for the classical, high order and two proposed elements with respect to the exact solutions with $NE=1$

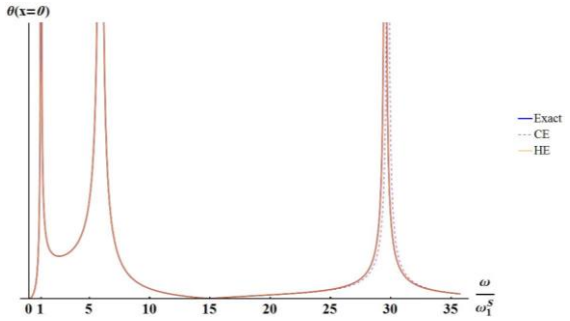

(a) *NE*=4

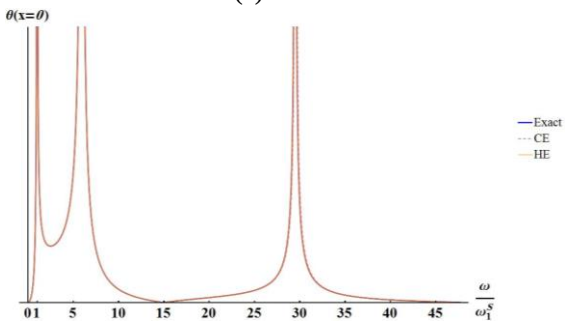

(b) *NE*=8

Fig. 8 FRFs for the classical and high order finite elements and the exact solutions

differences between two solutions, in higher frequencies this variation has still remained. For the sake of brevity, frequency response function curves for two proposed elements are not presented for the higher frequencies with the more number of elements since these curves are quite similar to those which are obtained from exact curves. As it is shown in Figs 7-8, the amplitude of frequency response function for unit harmonic ground excitation might be increased dramatically if the excitation frequency becomes close to the natural frequency due to the resonance phenomenon. While the resonance occurs, the vertical asymptotes can be observed in frequency response function curves.

As mentioned, the (SPE) is an alternative element for the classical element (CE). However, unlike what occurred in Fig. 7, (SPE) element converges to the higher frequencies rapidly and accurately in comparison with the (CE) element. Above figures lend plausible evidence to draw a conclusion that for the same number of elements and same values of ω/ω_1^s two proposed elements give more accurate and efficient solutions in contrast to those which are obtained from (CE) and (HE) elements. Although both proposed elements estimate the exact values similar to the high order element, the procedure for obtaining the results in these elements, eliminate the time-consuming steps of computations, considerably.

5. Conclusions

The main goal of this paper is to increase the efficiency and accuracy of the conventional elements by introducing two novel techniques. The traditional procedure of finding the interpolation functions of the classical beam element is expressed, briefly. As a common procedure by using the inner equidistant nodes with 2 degree of freedom at each node, the accuracy of the classical element is increased. In these methods, inversing the coefficient matrix includes the cumbersome and time-consuming step. To remedy this, two novel methods for diminishing the additional computational efforts are presented. The first proposed element (FPE), instead of utilizing traditional polynomials expression as a base function, taking the mode shapes of the clamped-clamped (C-C) beam into account. This means that, the upper right coefficient block becomes zero. The Second proposed element (SPE), utilizes not only the mode shapes of the clamped-clamped (C-C) beam as base functions but also considers *m* virtual degrees of freedom. In this case, both upper and lower right blocks become zero and the coefficient matrix is inverted straightforwardly. Afterwards, the reliability and sturdiness of both proposed elements are demonstrated via numerical examples. For this reason, free and forced vibrations of the generally restrained beam (GRB) are investigated. The obtained result through classical element indicate that the differences between exact solutions and this element. However, both proposed methods are able to estimate the exact solutions accurately. Besides, the results which are attained from the frequency response function curves have proven that the finite element solutions based on the high order element and both proposed elements could estimate the exact solutions more accurate in contrast to the classical element.

References

Abbas, B.A.H. (1984), "Vibrations of timoshenko beams with elastically restrained ends", *J. Sound Vib.*, **97**(4), 541-548.

Abu-Hilal, M. (2003), "Forced vibration of Euler-Bernoulli beams by means of dynamic green functions", *J. Sound Vib.*, **267**(2), 191-207.

Akgöz, B. and Civalek, O. (2014), "A new trigonometric beam model for buckling of strain gradient microbeams", *Int. J. Mech. Sci.*, **81**, 88-94.

Akgöz, B. and Civalek, O. (2015), "A novel microstructure-dependent shear deformable beam model", *Int. J. Mech. Sci.*, **99**, 10-20.

Anton, H. and Rorres, C. (2005), *Elementary linear algebra with applications*, (9th Edition), John wiley & Sons.

Augarde, C.E. (1998), "Generation of shape functions for straight beam elements", *Comput. Struct.*, **68**(6), 555-560.

Bishop, J.E. (2014), "A displacement-based finite element formulation for general polyhedra using harmonic shape functions", *Int. J. Numer. Method. Eng.*, **97**(1), 1-31.

Carrera, E., Pagani, A. and Petrolo, M. (2015), "Refined 1D finite elements for the analysis of secondary primary, and complete civil engineering structures", *J. Struct. Eng.*, **141**(4), 04014123.

Civalek, O. (2004), "Application of differential quadrature (DQ) and harmonic differential quadrature (HDQ) for buckling analysis of thin isotropic plates and elastic columns", *Eng. Struct.*, **26**(2), 171-186.

Civalek, O., Korkmaz, A. and Demir, C. (2010), "Discrete singular convolution approach for buckling analysis of rectangular Kirchhoff plates subjected to compressive loads on twoopposite edges", *Adv. Eng. Softw.*, **41**(4), 557-560.

Cook, R.D., Malkus, D.S. and Plesha, M.E. (1989), *Concepts and*

Applications of Finite Element Analysis, (3rd Edition), John Wiley & Sons, Singapore.
Dukić, E.P., Jelenić, G. and Gaćeša, M. (2014), "Configuration-dependent interpolation in higher-order 2D beam finite elements," *Finite Element Anal. Des.*, **78**, 47-61.
Greif, R. and Mittendorf, S.C. (1976), "Structural vibrations and fourier series", *J. Sound Vib.*, **48**(1), 113-122.
Gunda, J.B. and Ganguli, R. (2008), "New rational interpolation functions for finite element analysis of rotating beams", *Int. J. Mech. Sci.*, **50**(3), 578-588.
Hashemi, S.M. and Richard, M.J. (1999), "A new Dynamic Finite Element (DFE) formulation for lateral free vibrations of Euler-Bernoulli spinning beams using trigonometric shape functions", *J. Sound Vib.*, **220**(4), 578-588.
Hughes, T.J.R. (1987), *Finite Element Method: Linear Static and Dynamic Finite Element Analysis*, Prentice-Hall, New Jersey.
Inaudi, J.A. (2013), "Adaptive frequency-dependent shape functions for accurate estimation of modal frequencies", *J. Eng. Mech.*, **139**(12),1844-1855.
Kazakov, K.S. (2012), "Elastodynamic infinite elements based on modified bessel shape functions, applicable in the finite element method", *Struct. Eng. Mech.*, **42**(3), 353-362.
Kim, H.K. and Kim, M.S. (2001), "Vibration of beams with generally restrained boundary conditions using Fourier series", *J. Sound Vib.*, **245**(5), 771-784.
Kim, H.G. (2014), "A study on the development of shape functions of polyhedral finite elements", *J. Comput. Struct. Eng. Inst. Korea*, **27**(3), 183-189.
Li, T., Qi, Z., Ma, X. and Chen, W. (2015), "Higher-order assumed stress quadrilateral element for the Mindlin plate bending problem", *Struct. Eng. Mech.*, **54**(3), 393-417.
Liu, G.R. and Wu, T.Y. (2001), "Vibration analysis of beams using the generalized differential quadrature rule and domain decomposition", *J. Sound Vib.*, **246**(3), 461-481.
Macbai, J.C. and Genin, J. (1973), "Natural frequencies of a beam considering support characteristics", *J. Sound Vib.*, **27**(2), 197-206.
Milsted, M.G. and Hutchinson, J.R. (1974), "Use of trigonometric terms in the finite element method with application to vibrating membranes", *J. Sound Vib.*, **32**(3), 327-346.
Rao, C.K. and Mirza, S. (1989), "A note on vibrations of generally restrained beams", *J. Sound Vib.*, **130**(3), 453-465.
Rao, S.S. (2011), *The Finite Element Method in Engineering*, (5th Edition), Elsevier, Boston.
Reddy, J.N. (2006), *An Introduction to the Finite Element Method*, (3rd Edition), McGraw-Hill, Singapore.
Wang, J.T.S. and Lin, C.C. (1996), "Dynamic analysis of generally supported beams using Fourier series", *J. Sound Vib.*, **196**(3), 285-293.
Wang, X. and Yuan, Z. (2017), "Discrete singular convolution and taylor series expansion method for free vibration analysis of beams and rectangular plates with free boundaries", *Int. J. Mech. Sci.*, **122**, 184-191.